Analytic expressions for the electromagnetic mode density in finite, one-dimensional, photonic band-gap structures

Jon M. Bendickson* and Jonathan P. Dowling
Weapons Sciences Directorate, AMSMI-RD-WS-ST, Research, Development, and Engineering Center, U. S. Army Missile Command, Redstone Arsenal, Alabama 35898-5248

Michael Scalora
Department of Electrical Engineering, University of Alabama in Huntsville, Huntsville, Alabama 35899
(Received 13 September 1995)

We derive an exact expression for the electromagnetic mode density, and hence the group velocity, for a finite, N-period, one-dimensional, photonic band-gap structure. We begin by deriving a general formula for the mode density in terms of the complex transmission coefficient of an arbitrary index profile. Then we develop a specific formula that gives the N-period mode density in terms of the complex transmission coefficient of the unit cell. The special cases of mode-density enhancement and suppression at the photonic band edge and also at midgap, respectively, are derived. The specific example of a quarter-wave stack is analyzed, and applications to three-dimensional structures, spontaneous emission control, delay lines, band-edge lasers, and superluminal tunneling times are discussed.

PACS number(s): 41.20.Jb, 42.50.−p, 78.66.Fd, 85.60.Jb

I. INTRODUCTION AND BACKGROUND

In 1991 it was shown experimentally and theoretically that there exist three-dimensional, periodic, dielectric structures that exhibit an electromagnetic stop band for all polarizations and directions of photon propagation over a wide band of frequencies [1,2]. Since that time, a large class of such omnidirectional-Bragg-reflector geometries has been discovered [2], and they are usually referred to as photonic band-gap (PBG) "crystals." In general, elucidating the photonic band structure of such a three-dimensional (3D) crystal is an arduous task involving the computationally intensive eigenvalue problem for the solution of Maxwell's vector equations in a topologically complicated dielectric lattice [1,2]. Although such an approach yields very good agreement between theory and experiment [2], it has much to be desired for a simple analytical understanding of the electromagnetic properties of these materials.

One way to overcome this problem was provided by a model due to John and Wang [3], in which they approximate the 3D photonic crystal with a hypothetical structure that has a perfectly spherical Brillouin zone (BZ) for all polarizations. Although a geometry that yields such a BZ probably does not exist, the John-Wang model nevertheless reduces the intractable 3D problem to an analytically solvable 1D one, by producing a stop band that looks precisely the same for all polarizations and directions of photon propagation [3–5]. One drawback of this model, however, is the fact that for an *infinite* 1D PBG structure, the electromagnetic density of modes (DOM) becomes formally infinite at the photonic band edge, due to the low dimensionality of the system [4]. Since the mode density is proportional to the spontaneous emission rate of an embedded probe atom, by Fermi's "golden rule" [6], this restriction severely limits the usefulness of the John-Wang model in understanding the atomic emission enhancement expected at the photonic band edge.

In the current paper, we overcome this problem by developing an exact, analytical expression for the DOM of a *finite*, N-period, 1-D PBG lattice, in terms of the complex transmission coefficient $t(\omega)$ of a unit lattice cell. The restriction to a *finite* number of unit cells, periodically arrayed, removes the DOM singularity at the band edge. Our result is made possible by the combination of two recent discoveries in the 1D theory of scattering. Firstly, the complex transmission coefficient $t(\omega)$ of an arbitrary 1D scattering potential can be used to construct the group velocity, $v \equiv d\omega/dk$, and hence the DOM, $\rho \equiv dk/d\omega$, for that potential [7,8]. Secondly, for a finite, periodic, 1D PBG, there exists a compact analytic formula for the complex, N-cell, transmission coefficient t_N that can be written solely as a function of N, and the transmission coefficient $t(\omega)$ of the unit cell [9].

In addition to its application to the John-Wang model of a 3D PBG, our result has direct significance for understanding the DOM on axis in actual 1D distributed Bragg reflectors made from periodic, multilayered, dielectric stacks. So saying, our formulas can be used in the study of band-edge lasing [10]; band-edge spontaneous emission enhancement in layered semiconductors [7]; nonlinear optical effects such as gap solitons [11], bistability [12], limiting and switching [13], and thin-film optical isolators [14]. The fact that the N-period DOM, $\rho_N \equiv dk_N/d\omega$, is inversely proportional to the group velocity, $v_N = d\omega/dk_N$, allows us to also provide analytical statements about the group velocity slowdown at the photonic band edge, with applications to band-edge lasing [10] and optical delay lines [7], as well as about the anomalous group velocity at midgap, responsible for the recent observations of "superluminal" tunneling times [15,16].

In Sec. II we will review recent results that show, in general, how we may extract the DOM ρ for an arbitrary 1D scattering potential, or index profile $n(x)$, from the complex

*Permanent address: Department of Electrical Engineering, Auburn University, Auburn, AL 36849.

transmission coefficient $t(\omega)$ of that potential [7,8]. A review of the transmission properties of an arbitrary, N-cell, periodic potential is then discussed in Sec. III [9]. We combine these ideas in Sec. IV to produce our primary result: a general expression for the density of modes of an arbitrary N-period index potential, in terms of the complex transmission coefficient $t(\omega)$ of the unit period cell.

In Sec. V we illustrate these ideas by discussing N-period transmittance $T_N=|t_N|^2$ and DOM ρ_N curves in general, and then for the simple case of an N-period, quarter-wave, dielectric stack. Both $T_N(\omega)$ and $\rho_N(\omega)$ exhibit, in general, a remarkable series of N resonances in the first pass band, or $2N$ resonances in the higher-order bands, where the transmission is exactly unity—independently of the form of the unit cell t. In addition, at these resonances, the DOM is locally maximal. We shall discuss these resonances in Sec. VI, paying particular attention to the band-edge maximum. Here, we shall also consider the values of $T_N(\omega)$ and $\rho_N(\omega)$ at midgap while illustrating all these concepts again with the quarter-wave stack. We end, in Sec. VII, with the practical application of solving for the physical specifications of a particular stack whose band-edge, modal-resonance width matches a given fixed bandwidth $\Delta\omega$—say that of an embedded emitter. This result has direct application for optimizing the structure for maximal, band-edge, spontaneous emission enhancement [7]. In Sec. VIII we wind up with our summary and conclusions.

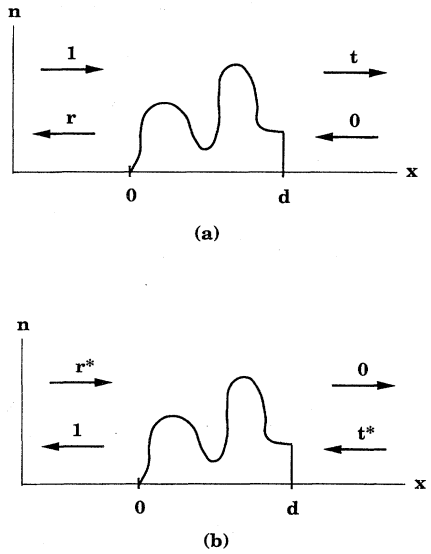

FIG. 1. In (a) we illustrate the scattering of light off a 1D, real index potential $n(x)$, where $x\in[0,d]$. The transmission and reflection coefficients are t and r, respectively, with $|t|^2+|r^2|=1$, by energy conservation. In (b) we show the time-reversed process of (a). The general transfer matrix, consistent with these processes, has the form of Eq. (11).

II. MODE DENSITY IN TERMS OF TRANSMISSION COEFFICIENT

There are several different conventions for defining the electromagnetic mode density $\rho(\omega)$ for a 1D index "potential" $n(x)$ [17]. We will use cavity QED to motivate the convention we use in this work. Suppose we have a lossless, dispersionless, index of refraction profile $n(x)$ that is nonzero over the interval $x\in[0,d]$ (see Fig. 1). The vector-potential, normal-mode eigenvectors for this profile, $a_k(x)$, obey the Helmholtz equation [4]

$$\frac{d^2a_k(x)}{dx^2}+\frac{\omega_k^2}{c^2}n^2(x)a_k(x)=0, \tag{1}$$

where c is the vacuum speed of light and ω_k is the eigenvalue, related to k via a dispersion relation, $k=k(\omega)$, that is determined as a part of the solution of Eq. (1). If an oscillating point dipole with frequency Ω_0 is embedded in the potential $n(x)$ at a point x_0, the inhomogeneous dielectric will alter the free-space emission rate. In particular, the emission rate γ (normalized to the free-space rate) is given by [4,7,18]

$$\gamma=\Omega_0|a_k(x_0)|^2\left.\frac{dk}{d\omega}\right|_{\omega=\Omega_0}, \tag{2}$$

where we normalize the eigenvectors a_k such that

$$\int_0^d a_{k'}^*(x)a_k(x)\,dx=\delta(k'-k). \tag{3}$$

From Fermi's "golden rule" [6], we know also—in the weak atom-cavity coupling limit—that the emission rate γ is proportional to the product of the atomic electric self-field intensity, $|E_k(x_0)|^2$, with the DOM, $\rho(\omega)$. Since $|E_k(x_0)|^2\propto|a_k(x_0)|^2$, then without loss of generality we may define

$$\rho(\omega)\equiv\frac{dk}{d\omega} \tag{4}$$

as our mode density. This convention has the natural interpretation that $\rho(\omega)$ is the number of wave numbers k per unit frequency ω, and hence it is the reciprocal of the group velocity [19], $v=1/\rho=d\omega/dk$. This velocity is associated with the propagation of a pulse peak through the potential $n(x)$. In addition, note that when ρ is large, the mean of $|a_k|^2$ will also be large—since then the group velocity is low and a quasi-standing wave forms in the structure [10]. Hence, a maximum of ρ will correspond to a maximum of the emission rate γ, provided that the dipole is located at an antinode of $|a_k(x)|^2$. Thus, knowledge of the density of modes can tell us much about the emission rate.

Now that we have motivated a reasonable definition of ρ, we need a simple way to compute it. A direct brute-force approach is to numerically solve the eigenvalue problem, Eq. (1), for the dispersion relation $k=k(\omega)$. However, we shall motivate here a faster and more elegant method that uses simple matrix-transfer techniques and one-dimensional scattering theory. Previous work has shown that the 1D scattering matrix can be used to derive the group velocity for a compact potential [8]. We now give a simple, physically intuitive derivation of that result [7]. Suppose, as in Fig. 1(a),

we have an electromagnetic wave of unit amplitude, and zero phase at $x=0$, incident from the left, as shown. Then the complex transmission coefficient amplitude on the right we will call $t(\omega)$, as indicated. Now, for optical applications such as thin films, usually one is only interested in the transmitted intensity or transmittance, $T\equiv|t|^2$. However, $t(\omega)$ also contains phase information, from which we can extract the dispersion relation $k=k(\omega)$ and hence the density of modes $\rho=dk/d\omega$, as we shall see.

Given the transmission coefficient for any structure, $t\equiv x+iy\equiv\sqrt{T}e^{i\varphi}$, it is simple to construct the density of modes. (Here, x is the real part of t and *not* the position coordinate.) We know that $\tan\varphi=y/x$, but φ is the total phase accumulated as the light propagates through the potential and hence can also be written as kd, where k is the effective wave number and d the physical thickness of the structure. Hence, the dispersion relation can be written as $\tan kd=y(\omega)/x(\omega)$. Therefore,

$$\frac{d}{d\omega}(\tan kd)=\frac{d}{d\omega}\left(\frac{y}{x}\right). \tag{5}$$

Evaluating the derivative of both sides yields

$$\sec^2(kd)\,\frac{dk}{d\omega}=\frac{1}{d}\,\frac{y'x-x'y}{x^2}, \tag{6}$$

where the prime denotes differentiation with respect to ω. After simplifying this expression with the identity $\tan^2\theta+1\equiv\sec^2\theta$ and solving for $dk/d\omega$, we get

$$\rho(\omega)\equiv\frac{dk}{d\omega}=\frac{1}{d}\,\frac{y'x-x'y}{x^2+y^2}. \tag{7}$$

It is significant to note that this equation is valid regardless of the spatial form of the potential $n(x)$ that we are dealing with. If we can find the real and imaginary parts of the transmission coefficients x and y, respectively, then we have all the necessary information to calculate the mode density ρ and group velocity $v=1/\rho$. From a computational point of view, the calculation of $t(\omega)=x+iy$ for a given potential $n(x)$ can be carried out quite simply by matrix-transfer techniques that are easily implemented numerically [7,19]. Then we take $x=\mathrm{Re}\{t\}$ and $y=\mathrm{Im}\{t\}$. In the practice of thin-film construction, $n(x)$ is a piecewise-constant function for which both $t(\omega)$ and the electric field profile in the structure, $E_\omega(x)$, can be readily obtained by matrix transfer [7,19]. Even if $n(x)$ is a continuous function, an approximation of $n(x)$ by a piecewise constant function, corresponding to a product of matrices, yields rapidly convergent values for $t(\omega)$ and $E_\omega(x)$ as the subdivision of $n(x)$ becomes sufficiently fine. Hence, all the information needed to compute the spontaneous emission rate γ, via formula (2), is available from a simple matrix-transfer solution to the 1D scattering problem. The density of modes, $\rho=dk/d\omega$, is obtained from $t=x+iy=\sqrt{T}e^{i\varphi}$, via Eq. (7), and the normal mode amplitudes $a_\omega(x)$ can be obtained from the hypothetical incident electric field profile $E_\omega(x)$ via the normalization

$$a_\omega(x)=\mathcal{N}_\omega E_\omega(x), \tag{8}$$

where

$$\mathcal{N}_\omega\equiv\left\{\int_0^d E_\omega^*(x)E_\omega(x)dx\right\}^{-1/2} \tag{9}$$

is the normalization constant, as required by Eq. (3). Precisely such a technique was used to analyze a recent experiment by our group on spontaneous emission rates at the photonic band edge of a GaAs/Ga_xAl_{1-x}As semiconductor 1D PBG [7].

Although a numerical matrix-transfer technique for computing the DOM is quite efficient for the general 1D problem, there is an understanding of scaling laws that can only be obtained from an analytical expression for ρ. An analytical solution for $t=x+iy$ would imply one for ρ, via Eq. (7). As we shall see in the next section, such a solution for $t(\omega)$ exists in the special case when $n(x)$ has the form of an N-period potential.

III. TRANSMISSION COEFFICIENT OF AN N-PERIOD POTENTIAL

Recent results in one-dimensional scattering theory have shown that the complex transmission coefficient $t_N(\omega)$ of an N-period periodic potential can be written, in general, in terms of $t(\omega)$, the transmission coefficient of a unit cell [9]. This result is remarkable in that the formula is nearly independent of the form of $t(\omega)$. We shall give a somewhat streamlined derivation of it here.

Let us start by deriving some properties of the scattering matrix for an arbitrary, dispersionless, real potential $n(x)$—not necessarily periodic—as shown in Fig. 1(a). In the interval $[0,d]$, the general solution to the Helmholtz equation (1) can be written as a superposition of right- and left-going waves, labeled plus and minus, respectively, as $u^{\pm}(x)=f^{\pm}(x)e^{\pm ikx}$, determined by the solution to Eq. (1). The $f^{\pm}$ are real envelope functions. Written in column vector form $\mathbf{u}=\binom{u^+}{u^-}$, we have the boundary conditions $\mathbf{u}(0)=\binom{1}{r}$ and $\mathbf{u}(d)=\binom{t}{0}$, by inspection of Fig. 1(a). If we define the transfer matrix $\hat{\mathbf{M}}=\binom{A\ B}{C\ D}$ via

$$\mathbf{u}(0)=\hat{\mathbf{M}}\mathbf{u}(d), \tag{10}$$

then the boundary conditions imply that $\binom{1}{r}=\binom{A\ B}{C\ D}\binom{t}{0}$, hence $A=1/t$ and $C=r/t$. Now for a complex wave $E\propto e^{ikx}$, the operation of time reversal $\hat{\tau}$ corresponds to complex conjugation; i.e., $\hat{\tau}(E)=E^*$. For real, linear, index profiles, the scattering process must be invariant under time reversal, yielding the process shown in Fig. 1(b). Thus, we read off a second boundary condition, namely, $\binom{r^*}{1}=\binom{A\ B}{C\ D}\binom{0}{t^*}$, or $B=r^*/t^*$ and $D=1/t^*$. This tells us that the scattering or transfer matrix $\hat{\mathbf{M}}$ for a real index profile must have the very general form

$$\hat{\mathbf{M}}=\begin{pmatrix}1/t & r^*/t^*\\ r/t & 1/t^*\end{pmatrix}. \tag{11}$$

If we also impose energy conservation, in the form $|r|^2+|t|^2\equiv R+T=1$, then it is easy to check that $\det|\hat{\mathbf{M}}|=1$, and hence $\hat{\mathbf{M}}$ is unimodular.

We digress here briefly to discuss the relationship between the operations of time-reversal $\hat{\tau}$ and parity $\hat{\pi}$. From Eq. (10) it is clear that $\hat{\mathbf{M}}_{\mathrm{RL}}\equiv\hat{\mathbf{M}}$ propagates right to left (RL)

across the potential $n(x)$. Hence, $\hat{\mathbf{M}}_{\mathrm{LR}} \equiv \hat{\mathbf{M}}_{\mathrm{RL}}^{-1}$ propagates left to right (LR). If we replace the transmission coefficient $t \rightarrow t_{\mathrm{LR}}$ in Eq. (11) for $\hat{\mathbf{M}}_{\mathrm{RL}} \equiv \hat{\mathbf{M}}$ and $t \rightarrow t_{\mathrm{LR}}$ in the equivalent of Eq. (11) for $\hat{\mathbf{M}}_{\mathrm{LR}}$ then t_{LR} can be found in terms of t_{RL} by constructing $\hat{\mathbf{M}}_{\mathrm{RL}}^{-1}$ via $\begin{pmatrix} A & B \\ C & D \end{pmatrix}^{-1} = \begin{pmatrix} D & -B \\ -C & A \end{pmatrix}$, since $\det|\hat{\mathbf{M}}| = 1$. Reading off the diagonal terms of the equation $\hat{\mathbf{M}}_{\mathrm{RL}}^{-1} = \hat{\mathbf{M}}_{\mathrm{LR}}$, we find $t_{\mathrm{RL}}^* = t_{\mathrm{LR}}$ or $T_{\mathrm{RL}} = |t_{\mathrm{RL}}^*|^2 = |t_{\mathrm{LR}}|^2 = T_{\mathrm{LR}}$. Hence, the one-dimensional transmittance T is invariant under the parity operation $\hat{\pi}(T_{\mathrm{RL}}) = T_{\mathrm{LR}} = T_{\mathrm{RL}} \equiv T$. This is a direct consequence of the assumptions of energy conservation, time-reversal symmetry, and the fact that the index potential $n(x)$ is real and linear. If $n(x)$ is complex—indicating the presence of absorption or gain—or if $n(x)$ contains nonlinear Kerr media, and hence is intensity dependent, then time-reversal still holds, but it no longer implies parity conservation in transmittance. [For a Kerr medium, the solutions on opposite sides of $n(x)$ are no longer related by a linear matrix transformation.] This fact is used in the thin-film, Kerr-nonlinear, optical diode or isolator that exhibits an anisotropic transmittance [14].

The eigenvalue equation for $\hat{\mathbf{M}}$ is easily seen from Eq. (11) to be

$$\mu^2 - 2\mu \ \mathrm{Re}\{1/t\} + 1 = 0, \tag{12}$$

where the two eigenvalues $\mu^{\pm}$ are related by $\mu^+ \mu^- = \det|\hat{\mathbf{M}}| = 1$ by unimodularity.

We now would like to make a very important point. Suppose, for the sake of discussion, we were to impose the periodic boundary condition, $n(x) = n(x+d)$, for $x \in (-\infty, \infty)$, and then seek the corresponding Bloch eigenfunctions $\mathbf{u}_B$, appropriate for an *infinite*-period potential with unit cell $n(x)$, $x \in (0,d]$. We know that the Bloch functions change only in phase—and not in amplitude—from cell to cell in the infinite periodic potential. This phase per unit cell is called the *Bloch phase* β, associated with the infinite periodic structure [4,17]. (This is *not* the same as the phase φ associated with the unit cell transmission coefficient, $t = \sqrt{T} e^{i\varphi}$.) For these Bloch eigenfunctions $\mathbf{u}_B$, we have then—from the definition of *eigenvector*—the *eigenvector equation*

$$\hat{\mathbf{M}} \mathbf{u}_B = \mu_B^{\pm} \mathbf{u}_B = e^{\pm i\beta} \mathbf{u}_B, \tag{13}$$

where the last term comes from the definition of the Bloch phase β. Hence, the eigenvalues for the Bloch functions are of the form $\mu_B^{\pm} = e^{\pm i\beta}$, since $\mu_B^+ \mu_B^- = 1$. Now, since the eigenvalue equation (12) holds for all eigenvalues μ of $\hat{\mathbf{M}}$, in particular it holds for the $\mu_B^{\pm}$. Inserting $\mu_B^{\pm} = e^{\pm i\beta}$ into (12), and equating real and imaginary terms, yields the very important relation that

$$\mathrm{Re}\{1/t\} = \cos\beta, \tag{14}$$

where β is again the Bloch phase for the hypothetical infinite periodic structure. This will be crucial to remember later in this work.

Let us go back now to the single-unit potential $n(x)$, $x \in (0,d]$, Fig. 1. We note from the Cayley-Hamilton theorem [20], which states that every matrix obeys its own eigenvalue equation, that we can use Eqs. (12) and (14) to write

$$\hat{\mathbf{M}}^2 - 2\hat{\mathbf{M}} \cos\beta + \hat{\mathbf{I}} = 0. \tag{15}$$

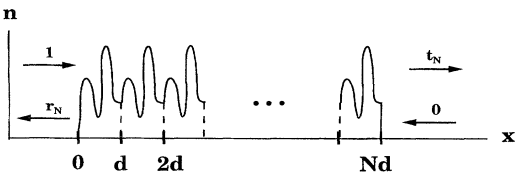

FIG. 2. Here we take the unit-cell potential $n(x)$ of Fig. 1 and repeat it N times to obtain the N-period, finite, periodic potential, $n(x) = n(x+d)$, where $x \in [0,Nd]$. Here, t_N and r_N are the N-period coefficients, with $|t_N|^2 + |r_N|^2 = 1$. The N-period transfer matrix $\hat{\mathbf{M}}^N$ is given in terms of the unit cell $\hat{\mathbf{M}}$ by Eq. (16) and has the general form of Eq. (17).

Then, by induction (see Appendix A), it is easy to establish that the transfer matrix $\hat{\mathbf{M}}^N$ for a *finite*, N-period potential, of unit cell $n(x)$, is given by

$$\hat{\mathbf{M}}^N = \hat{\mathbf{M}} \frac{\sin N\beta}{\sin\beta} - \hat{\mathbf{I}} \frac{\sin(N-1)\beta}{\sin\beta}, \tag{16}$$

where $\hat{\mathbf{I}}$ is the unit matrix (see Fig. 2). Hence, we arrive at the important result that the scattering (or transfer) matrix $\hat{\mathbf{M}}^N$ for an N-period potential can be written simply in terms of the unit cell matrix $\hat{\mathbf{M}}$, the number of periods N, and the Bloch phase β that is normally associated with the *infinite* periodic potential.

It is now an easy task to compute the complex transmission coefficient t_N for the N-period structure. The general form of the transfer matrix derived for $\hat{\mathbf{M}}$, Eq. (11), also holds for any such matrix, including $\hat{\mathbf{M}}^N$. In particular, we have

$$\hat{\mathbf{M}}^N = \begin{pmatrix} 1/t_N & r_N^*/t_N^* \\ r_N/t_N & 1/t_N^* \end{pmatrix}. \tag{17}$$

Now let us take these expressions for $\hat{\mathbf{M}}$ and $\hat{\mathbf{M}}^N$, Eqs. (11) and (17), and insert them into the matrix equation (16). By considering firstly the diagonal and then secondly the off-diagonal terms, respectively, we get

$$\frac{1}{t_N} = \frac{1}{t} \frac{\sin N\beta}{\sin\beta} - \frac{\sin(N-1)\beta}{\sin\beta}, \tag{18a}$$

$$\frac{r_N}{t_N} = \frac{r}{t} \frac{\sin N\beta}{\sin\beta}. \tag{18b}$$

For our DOM calculation in the next section, we will use the complex transmission coefficient $t_N = \sqrt{T_N} e^{i\varphi_N}$, Eq. (18a), to extract the phase information φ_N needed to obtain the DOM,

ρ_N. The N-period transmittance, $T_N \equiv |t_N|^2$, is most easily obtained by taking the modulus squared of Eq. (18b) and applying conservation of energy in the form $|r|^2 = 1 - |t|^2$, or $R = 1 - T$. This yields

$$\frac{1}{T_N} = 1 + \frac{\sin^2 N\beta}{\sin^2 \beta}\left[\frac{1}{T} - 1\right]. \tag{19}$$

These results for a general N-period potential are the same as given by Sprung, Wu, and Martorell (SWM) [9]. Equation (19) has also been derived by Yariv and Yeh, in the special case where the unit cell is composed of a two-layer step index profile [19]. Once again, the phase β here is the Bloch phase of the $N=\infty$ structure, given by Eq. (14), and *not* either of the phases φ_N or φ associated with the N-period or unit-cell potential, respectively.

In general, we see that the infinite-period Bloch phase β plays a very important role in the finite-period structure. In particular, the passbands and stop bands of the N-period potential mirror very closely those of the infinite lattice. The Bloch phase will be real whenever $|\mathrm{Re}\{1/t\}| \leq 1$ and complex otherwise, corresponding to the passband and band-gap conditions, respectively. In the gap, we set $\beta = i\theta$ or $\beta = \pi + i\theta$, depending on whether $\mathrm{Re}\{1/t\} > 1$ or $\mathrm{Re}\{1/t\} < -1$, respectively. Notice that in the passbands T_N varies sinusoidally with β. We have $\beta \in [0,\pi]$ in the first band, $\beta \in [\pi, 3\pi]$ in the second, and so forth. From the identity, $\sin^2\theta = (1-\cos 2\theta)/2$, we see from Eq. (19) that T_N is periodic in β with period π/N, and hence we expect it to exhibit N oscillations in each passband interval of β length π.

Inside the gap, where β is complex, we shall see that all the sinusoidal behavior changes into a hyperbolic exponential form. More of the properties of T_N will be covered in Sec. VI. What is remarkable is that many of the interesting properties of T_N are qualitatively independent of the form of the unit cell's transmission T. This indicates that most of the rich structure arising in the transmission and DOM of a periodic potential arises purely from the finite periodicity, independent of the form of the unit cell.

IV. DERIVATION OF MODE DENSITY AND GROUP VELOCITY FOR AN N-PERIOD STRUCTURE

We will define the N-period mode density as $\rho_N = dk_N/d\omega$ and the group velocity as $v_N = 1/\rho_N = d\omega/dk_N$. Given the transmission coefficient for the structure, $t_N = x_N + iy_N = \sqrt{T_N} e^{i\varphi_N}$, it is simple to construct the density of modes using Eq. (7), derived in Sec. II (see Fig. 2).

We will now make use of the results of Sprung, Wu, and Martorell [9], summarized in Sec. III above, by using Eqs. (14) and (18a) for $\cos\beta$ and t_N as a starting point. For these two equations, $t_N(\omega)$ refers to the complex transmission coefficient for the N-period structure (Fig. 2), and $t(\omega)$ refers to the transmission coefficient for a single period (Fig. 1), with x and y being t's real and imaginary parts, respectively. After performing some algebraic manipulations on Eq. (18a), it is possible to solve for the real and imaginary parts of t_N, namely, x_N and y_N, respectively, in terms of $t = x + iy$ for the unit cell. We get

$$x_N = \frac{x \sin N\beta \sin\beta - (x^2+y^2)\sin\beta \sin(N-1)\beta}{\sin^2 N\beta - 2x \sin N\beta \sin(N-1)\beta + (x^2+y^2)\sin^2(N-1)\beta}, \tag{20a}$$

$$y_N = \frac{y \sin N\beta \sin\beta}{\sin^2 N\beta - 2x \sin N\beta \sin(N-1)\beta + (x^2+y^2)\sin^2(N-1)\beta}, \tag{20b}$$

where $\cos\beta = \mathrm{Re}\{1/t\}$, as before. Because x_N and y_N are fairly complicated functions of β, x, and y—that are themselves all functions of frequency ω—a direct calculation of ρ_N at this point, via the differentiations required by Eq. (7), would be somewhat unmanageable. However, the problem simplifies significantly by making the substitution $z_N = y_N/x_N$.

From Sec. III we know that $\varphi_N = k_N D = \tan^{-1}(z_N)$, and hence,

$$\rho_N \equiv \frac{dk_N}{d\omega} = \frac{1}{D}\frac{d}{d\omega}\tan^{-1}(z_N) = \frac{1}{D}\frac{z_N'}{1+z_N^2}, \tag{21}$$

where $D = Nd$ is the length of the N-period potential. Since Eqs. (20a) and (20b) for x_N and y_N have the same denominator, the expression for z_N simplifies to

$$z_N = \frac{y \sin N\beta}{x \sin N\beta - (x^2+y^2)\sin(N-1)\beta}. \tag{22}$$

By making the substitution for the unit-cell transmission coefficient, $T = x^2 + y^2$, and the scaled quantities $\xi = x/T$, and $\eta = y/T$, then z_N can be further simplified. The fact that $\xi = \cos\beta$ will also be used in the simplification, which eventually yields

$$z_N = z \tan N\beta \cot\beta, \tag{23}$$

where $z \equiv y/x$ corresponds to the unit cell. Note that this implicitly gives the dispersion relation $k_N = k_N(\omega)$ for the stack in the form $\tan\varphi_N = \tan(k_N D) = z_N = z \tan N\beta \cot\beta$. Now, we can use this expression for z_N with Eq. (21) to calculate the mode density ρ_N. After some algebraic manipulation we get

$$\rho_N=\frac{1}{D}\,\frac{(1/2)[\sin(2N\beta)/\sin\beta][\,\eta'+\eta\xi\xi'/(1-\xi^2)]-N\eta\xi'/(1-\xi^2)}{\cos^2N\beta+\eta^2[\sin(N\beta)/\sin\beta]^2}, \tag{24}$$

where $D=Nd$. This is our primary result for this paper. Here we have an exact expression for the density of modes of the N-period potential in terms of the number of periods N, the Bloch phase β, and the transmission coefficient t of the unit cell. Up to this point, no assumptions have been made concerning the actual spatial variation of the index $n(x)$ of the unit cell.

V. QUARTER-WAVE STACK

For a quarter-wave stack there is a fixed relationship between the indices of refraction n_1 and n_2, and the thicknesses of the layers, a and b, respectively, in the periodic structure, as illustrated in Fig. 3. Each layer is designed so that the optical path is exactly 1/4 of some reference wavelength λ_0 corresponding to the midgap frequency ω_0. From this fact, we can write

$$n_1a=n_2b=\frac{\lambda_0}{4}=\frac{\pi c}{2\omega_0}. \tag{25}$$

Next, we will calculate the transmission function and density of modes for a finite quarter-wave stack. We will first develop an expression for the quarter-wave unit-cell transmission coefficient $t^{\lambda/4}$ using formulas from Appendix B. Doing this, we get from Eq. (B9a), the complex transmission coefficient of an arbitrary two-layer unit cell, namely,

$$t=\frac{T_{12}e^{i(p+q)}}{1-R_{12}e^{2iq}}, \tag{26}$$

where

$$T_{12}=t_{12}t_{21}=\frac{4n_1n_2}{(n_1+n_2)^2} \tag{27a}$$

and

$$R_{12}=(r_{12})^2=\left(\frac{n_1-n_2}{n_1+n_2}\right)^2 \tag{27b}$$

are the double-transmission and reflection factors, defined as per Eq. (B3). Here, $p=n_1a\omega/c$ and $q=n_2b\omega/c$, where Eq. (25) holds in addition for a quarter-wave stack. Note that $T_{12}+R_{12}=1$. After extracting the real and imaginary parts from the quarter-wave cell transmission coefficient, $t^{\lambda/4}$, we have unit-cell expressions for $x^{\lambda/4}$ and $y^{\lambda/4}$,

$$x^{\lambda/4}=T_{12}\,\frac{\cos\pi\tilde{\omega}-R_{12}}{1-2R_{12}\cos\pi\tilde{\omega}+R_{12}^2}, \tag{28a}$$

$$y^{\lambda/4}=T_{12}\,\frac{\sin\pi\tilde{\omega}}{1-2R_{12}\cos\pi\tilde{\omega}+R_{12}^2}, \tag{28b}$$

where $\tilde{\omega}\equiv\omega/\omega_0$, with ω_0 at midgap. The unit-cell transmission, $T\equiv t^*t$, becomes

$$T^{\lambda/4}=\frac{T_{12}^2}{1-2R_{12}\cos\pi\tilde{\omega}+R_{12}^2}. \tag{29}$$

Finally, we can now calculate all of the components necessary to derive $\rho_N^{\lambda/4}$ via Eq. (24). Using $\xi\equiv x/T$ and $\eta\equiv y/T$, we have

$$\cos\beta=\xi=\frac{\cos\pi\tilde{\omega}-R_{12}}{T_{12}}, \tag{30a}$$

$$\eta=\frac{\sin\pi\tilde{\omega}}{T_{12}}, \tag{30b}$$

$$\xi'=-\frac{\pi}{\omega_0}\,\frac{\sin\pi\tilde{\omega}}{T_{12}}, \tag{30c}$$

$$\eta'=\frac{\pi}{\omega_0}\,\frac{\cos\pi\tilde{\omega}}{T_{12}}, \tag{30d}$$

where Eq. (30a) for ξ also determines the Bloch phase β. In Figs. 4 and 5 we plot the transmission T_N and ρ_N together, for $n_1=1$; $n_2\in\{\sqrt{2},2\}$, and $N\in\{5,10\}$, to illustrate the general behavior. We normalize ρ_N to the dimensionless quantity $v^{\text{bulk}}\rho_N$, where we define the bulk group velocity,

$$v^{\text{bulk}}\equiv(c/2)[1/n_1+1/n_2], \tag{31}$$

defined as the distance d over the travel time, discounting reflections. From Figs. 4 and 5 we can see a number of interesting properties of the transmission coefficient and mode density. First of all we know that for an N-period structure there are exactly N peaks to the left of the first gap in both the transmission coefficient and mode-density curves, since both T_N and ρ_N are periodic in β with period π/N, and in the first passband $\beta\in[0,\pi]$. We can also see that as n_2 and N are increased, the band gap becomes more sharply defined approaching the $N\to\infty$ limit, and the band-edge peaks of the mode-density curve are larger. The maxima and minima of

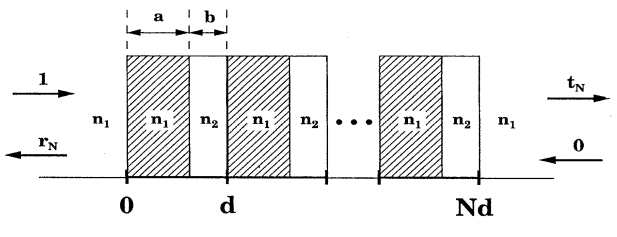

FIG. 3. Here we show the general, N-period stack composed of two-layer unit cells of thicknesses a and b and constant, real indices n_1 and n_2, respectively. If, in addition, $a=\lambda_0/(4n_1)$ and $b=\lambda_0/(4n_2)$, where λ_0 is some reference wavelength, then we have a quarter-wave stack whose first band gap is centered about λ_0, as per Eq. (25).

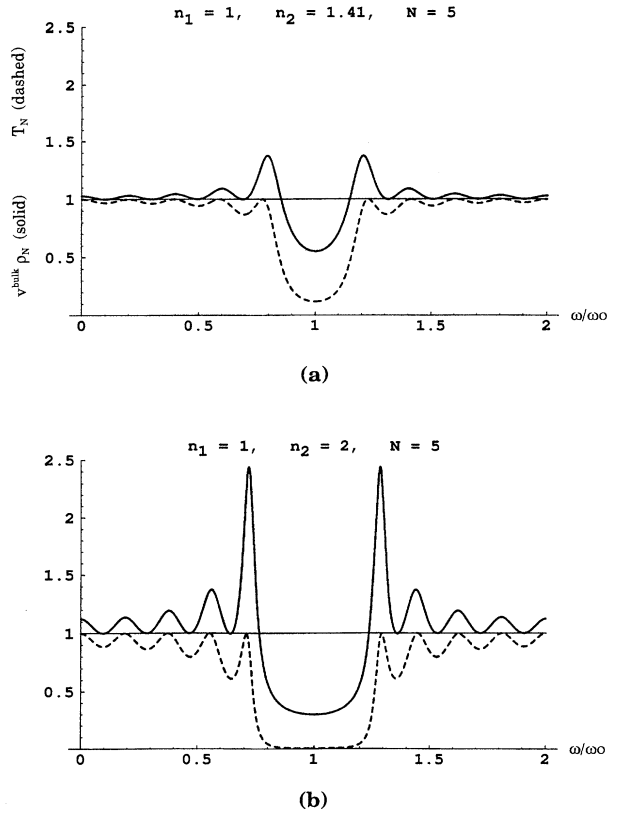

FIG. 4. Plot of the dimensionless DOM, $v^{\text{bulk}}\rho_N$—normalized to v_{bulk}—Eqs. (24) and (30) (solid) and the dimensionless transmittance T_N, Eq. (29) (dashed) vs dimensionless frequency ω/ω_0 for a five-period ($N=5$), quarter-wave stack with (a) $n_1=1$, $n_2=1.41$; and (b) $n_1=1$, $n_2=2$. Notice the five transmission resonances on either side of the band gap in both plots, corresponding to $N=5$. As the value of n_2 increases (b), the gap becomes more defined and the DOM resonances are greater in magnitude. The maxima and minima of the DOM and transmission appear to line up; however, there is a small amount of offset between the extreme values of the two curves that becomes rapidly negligible for increasing number of periods N.

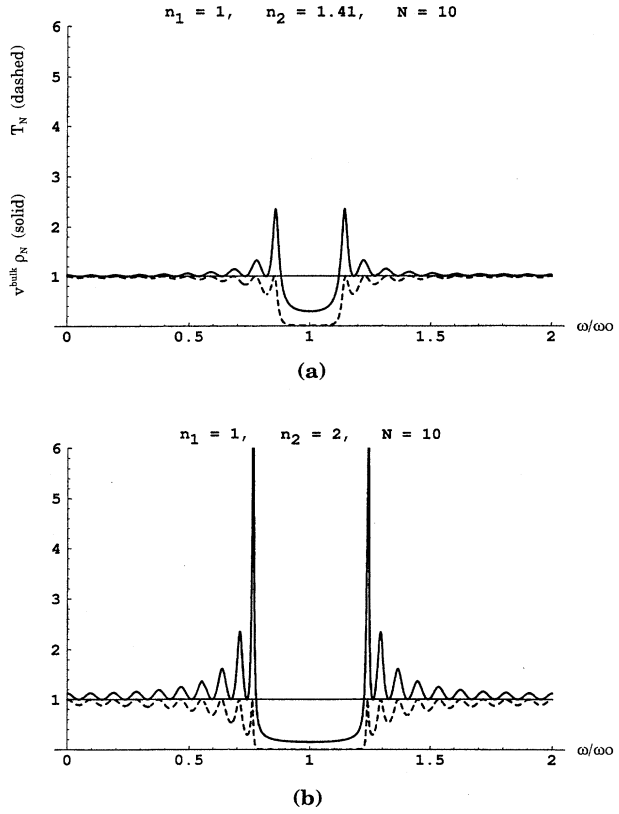

FIG. 5. Plot of the dimensionless DOM, $v^{\text{bulk}}\rho_N$, Eqs. (24) and (30) (solid) and dimensionless transmission T_N, Eq. (29) (dashed) vs dimensionless frequency ω/ω_0, for a 10-period, quarter-wave stack with (a) $n_1=1$, $n_2=1.41$, and (b) $n_1=1$, $n_2=2$. There are now $N=10$ transmission resonances on either side of the band gap, as opposed to the $N=5$ in Fig. 4. Notice also that an increase in the number of layers increases the magnitude of the DOM band resonances, and decreases the DOM in the band gap.

the two curves appear to line up with one another. However, there is actually some offset between these extreme values that becomes rapidly negligible with increasing N. All of these points will be covered in more detail in the next section.

VI. PROPERTIES OF T_N AND ρ_N

In this section we take a closer look at the formulas for the transmittance T_N and the DOM ρ_N, Eqs. (19) and (24), respectively, for an N-period potential, as shown in Fig. 2. To begin with, we analyze the transmission formula, summarizing and expanding on the results of SWM [9] and Yeh [19]. From Eq. (19) for T_N, we know that whenever $N\beta=m\pi$, $m\in\{0,1,\ldots,N-1\}$, then the $\sin^2 N\beta$ term is equal to zero and $T_N=1$, exactly. This phenomenon corresponds to the N transmission resonances seen in Figs. 4 and 5. What is remarkable is that, in general, these transmission resonances of T_N are unity—*independent* of the unit cell's transmission T. In other words, even if $T(\omega)$ is practically zero at these points—and hence the unit cell highly reflective—nevertheless the entire N-period stack is absolutely transparent. These "sweet spots" are hence properties of the finite periodicity of the stack alone, not of the unit cell. These resonances are well known in the theory of periodic, multilayered, thin films [19]—but the fact that they are a general property of *any* N-period 1D dielectric structure has not been fully appreciated [9]. In addition, Brown and McMahon have recently observed similar resonances in transmission experiments with finite 3D PBG crystals, while Pendry and coworkers have also predicted them in 2D and 3D transmission calculations [21], indicating that the phenomenon generalizes to higher-dimensional lattices. A study of such transmission or tunneling resonances has been made in 1D by Yeh, in the context of light propagation through finite, periodic, $GaAs/Al_xGa_{1-x}As$ heterostructures with steplike unit-cell index profiles [19]. Yeh argues that these resonances are consequences of the transverse guided modes that propagate in the y and z directions of the physical, layered, "1D" structure, by comparing our Eq. (19) for T_N to the dispersion

equation for the guided modes, which is similar to our Eq. (18a). However, our calculation made here of these T_N resonances is from a strictly 1D scattering theory, and hence casts doubt on this interpretation. It is our position that these resonances are strictly one-dimensional effects, and that physically they have nothing to do with the transverse guided-wave modes. In particular, these resonances are predicted to appear in true 1D systems—such as for electron waves in periodically modulated quantum wires—where clearly no transverse guided modes are present [22].

When $N\beta$ is equal to odd multiples of $\pi/2$, for example, $N\beta=(2m+1)\pi/2$, then the transmission curve T_N will be close to, but not exactly at, a local minimum [9]. This approximation improves very rapidly with increasing N. This is due to the fact that $\sin^2 N\beta$ is a maximum at this point, and since it is the most rapidly varying term, the entire function will be close to its minimum, as can be seen from Eq. (19). If we evaluate T_N at these approximate minima points, we find that

$$\left.\frac{1}{T_{\min}}\right|_{\beta=[(2m+1)/N]\pi/2} \cong 1+\frac{1}{\sin^2[(2m+1)\pi/2N]}\left[\frac{1}{T}-1\right]. \tag{32}$$

For a quarter-wave stack, this expression can be simplified. In general, the transmission coefficient $T_N^{\lambda/4}(\omega)$ for the quarter-wave stack is

$$T_N^{\lambda/4}=\frac{1+\cos\beta}{1+\cos\beta+2(R_{12}/T_{12})\sin^2 N\beta}, \tag{33}$$

where T_{12} and R_{12} are defined in Sec. V, Eq. (27), and β implicitly by Eq. (30a). The minima for the quarter-wave stack can then be written as

$$T_N^{\lambda/4-\min}=\frac{1+\cos[(2m+1)\pi/2N]}{1+2R_{12}/T_{12}+\cos[(2m+1)\pi/(2N)]}. \tag{34}$$

A final expression for the transmission minima that could be useful is an approximation for the band-edge minimum for large values of N. At this point, $\beta=\pi(2N-1)/(2N)$ or $m=N-1$. By writing a Taylor series expansion for the cosine terms in Eq. (34), we get the relation

$$T_N^{\lambda/4-\min}|_{m=N-1} \underset{N\to\infty}{\sim} \frac{\pi^2}{16}\frac{T_{12}}{R_{12}}\frac{1}{N^2}, \tag{35}$$

where T_{12} and R_{12} are given by Eq. (27). This expression shows that the minimum between the left band-edge resonance and the $N=\infty$ band edge decreases proportionally to $1/N^2$, Fig. 6(a), showing how fast the gap wall is approaching the step function of $N=\infty$.

Another region of interest for the transmission function T_N is inside the band gap. It is well known that inside the first band gap, the Bloch phase has the form $\beta=\pi+i\theta$ [9,19]. By using this fact, and converting sines and cosines to their hyperbolic equivalents via $\sin i\theta=i\sinh\theta$ and $\cos i\theta=\cosh\theta$, we obtain

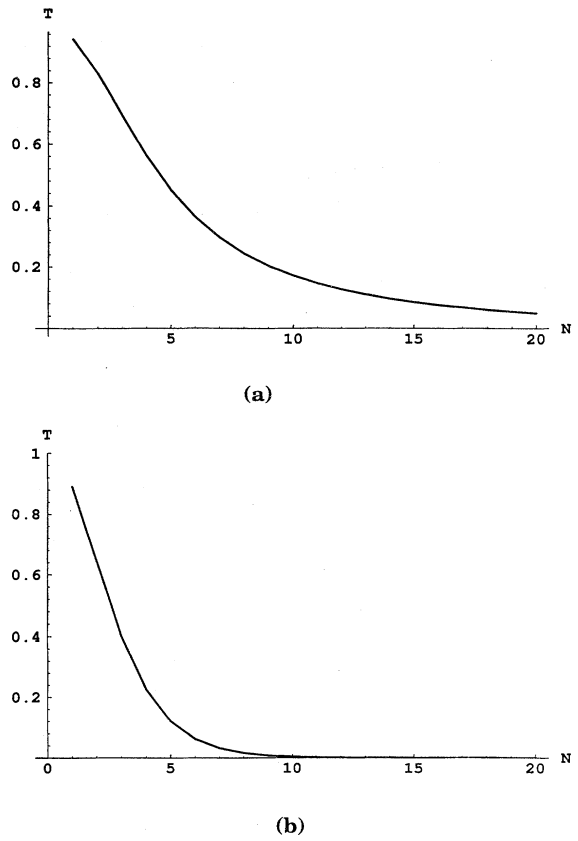

FIG. 6. Plot of (a) the dimensionless band-edge minimum of the transmission $T_N^{\lambda/4-\min}$, Eq. (35), and (b) the dimensionless midgap transmission $T_N^{\lambda/4-\mathrm{MG}}$, Eq. (40), vs the number of periods N for a quarter-wave stack with $n_1=1$ and $n_2=1.41$. The band-edge transmission minimum illustrates how fast the transmission curve approaches the $N=\infty$ step function. We observe a $1/N^2$ relationship between the band-edge transmission minimum and the number of periods N. For the midgap transmission we see an exponential decrease in transmission vs the number of periods.

$$\frac{1}{T_N^{\mathrm{gap}}}=1+\frac{\sinh^2 N\theta}{\sinh^2\theta}\left(\frac{1}{T}-1\right), \tag{36}$$

where $\theta=\cosh^{-1}(-\xi)$. This is a general formula for T_N anywhere in the band gap. For the specific case of a quarter-wave stack we can express the gap transmittance as

$$T_N^{\lambda/4-\mathrm{gap}}=\frac{\sinh^2\theta/2}{\sinh^2\theta/2+(R_{12}/T_{12})\sinh^2 N\theta}. \tag{37}$$

At exactly midgap $\tilde{\omega}=\omega/\omega_0=1$, so for the quarter-wave stack we have, at midgap (MG), $\cos\beta^{\mathrm{MG}}=-\cosh\theta^{\mathrm{MG}}=(\cos\pi-R_{12})/T_{12}$, which implies

$$\theta^{\mathrm{MG}}=\cosh^{-1}\left(\frac{1+R_{12}}{T_{12}}\right)=\ln\nearrow, \tag{38}$$

where $\nu = n_i/n_j$, with $n_i < n_j$ and $i,j \in \{1,2\}$. Evaluating T_N^{gap} at midgap for a quarter-wave stack yields, then,

$$T_N^{\lambda/4-\text{MG}} = \frac{1}{1+\sinh^2 N\theta^{\text{MG}}}, \tag{39}$$

which can be simplified to

$$T_N^{\lambda/4-\text{MG}} = \frac{1}{1+(1/4)[\nu^N - \nu^{-N}]^2}, \tag{40}$$

where $\nu = n_1/n_2$ or n_2/n_1.

This last equation can be approximated asymptotically by making a Taylor series expansion that is valid for large N. If this is done, then

$$T_N^{\lambda/4-\text{MG}} \underset{N\to\infty}{\sim} 4\nu^{2N}, \tag{41}$$

$\nu = n_i/n_j$, where $n_i < n_j$. So then we observe asymptotically an *exponential* decrease in the midgap transmission coefficient for increasing values of N. [See Fig. 6(b).]

Now that we have analyzed the transmission function in detail, we will follow the same general procedure for the density of modes ρ_N. To begin with, we use the fact that the peaks of T_N and ρ_N very nearly line up, with the approximation improving rapidly with increasing N [9], so that the density of modes in the left passband will have its maxima at approximately $\beta = m\pi/N$, $m \in \{0,1,\ldots,N-1\}$. This can be understood by inspecting Eq. (24) for ρ_N, where we see that when $N = m\pi$, then $\sin N\beta = 0$, $\sin 2N\beta = 0$, and $\cos^2 2N\beta = 1$. Hence, the most rapidly varying term in the denominator of ρ_N is nearly as small as possible, while the numerator remains proportional to large N—tending to maximize ρ_N. Evaluating the density of modes at these approximate maxima gives the general equation

$$\rho_N^{\max}|_{\beta = m\pi/N} \cong -\frac{1}{D}\frac{N\eta\xi'}{1-\xi^2}\bigg|_{\beta = m\pi/N}. \tag{42}$$

For the case of the quarter-wave stack, the expression can be simplified using Eqs. (30) for ξ and η, and by making the substitution $D = Nd$ where N is the number of periods and d is the physical thickness of a single period. The parameter d does not appear in the equation below, because for a quarter-wave stack it can be expressed in terms of ω_0, n_1, and n_2 via

$$d = \frac{\pi c}{2\omega_0}\left(\frac{n_1+n_2}{n_1 n_2}\right) = \frac{\pi}{\omega_0} v^{\text{bulk}}, \tag{43}$$

where v^{bulk} is defined in Eq. (31). Hence, the DOM maxima can be written as

$$\rho_N^{\lambda/4-\max}|_{\beta = m\pi/N} \cong \frac{1}{v^{\text{bulk}}}\frac{1 - T_{12}\sin^2[m\pi/(2N)]}{T_{12}\cos^2[m\pi/(2N)]}, \tag{44}$$

where T_{12} is given by Eq. (27a). The maximum of the density of modes nearest the band edge is of special interest for a variety of applications. For this case, we use the fact that $m = N-1$ at the band-edge resonance (BER), resulting in the formula

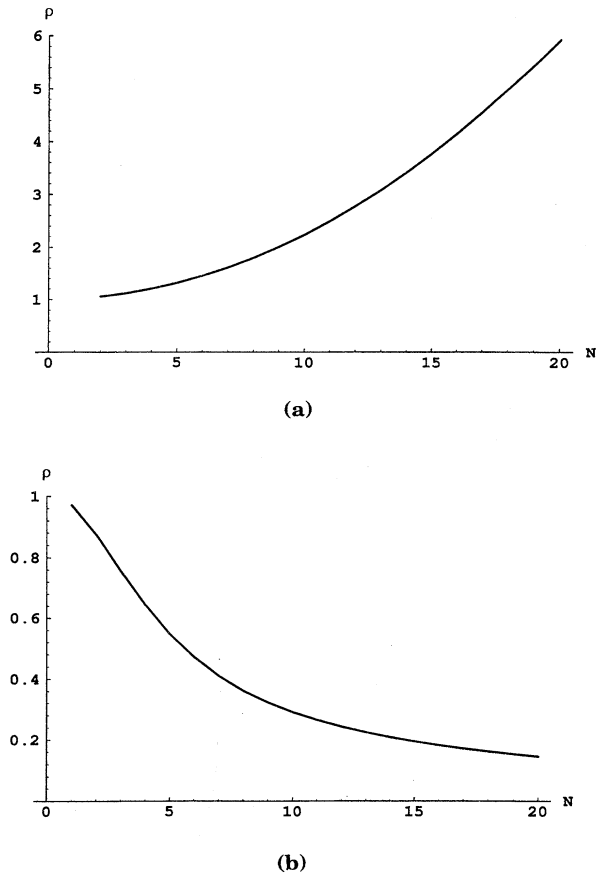

FIG. 7. Plot of (a) the dimensionless band-edge resonance DOM $v^{\text{bulk}}\rho_N^{\lambda/4-\text{BER}}$, Eq. (45), and (b) the dimensionless midgap DOM $v^{\text{bulk}}\rho_N^{\text{MG}}$, Eq. (48), vs the number of periods N for a quarter-wave stack with $n_1 = 1$ and $n_2 = 1.41$. The DOM maximum at the band edge increases proportionally to N^2 for fixed n_1 and n_2 and moderately large values of N. At midgap, the DOM is asymptotically inversely proportional to the number of periods N.

$$\rho_N^{\lambda/4-\text{BER}}|_{\beta = \pi - \pi/N} \cong \frac{1}{v^{\text{bulk}}}\frac{1 - T_{12}\cos^2[\pi/(2N)]}{T_{12}\sin^2[\pi/(2N)]}. \tag{45}$$

Again, we can use a Taylor series to give us an asymptotic approximation valid for large values of N,

$$\rho_N^{\lambda/4-\text{BER}} \underset{N\to\infty}{\sim} \frac{4}{\pi^2 v^{\text{bulk}}}\frac{R_{12}}{T_{12}}N^2. \tag{46}$$

For moderately large N, we can see that $\rho_N^{\lambda/4-\text{BER}}$ increases proportionally to N^2, an important point for band-edge emission enhancement and delay-line applications [4,7]. [See Fig. 7(a).] Finally, we take a look at what happens to the mode density for frequencies inside the band gap. Because in the first gap $\beta = \pi + i\theta$, we can replace the trigonometric terms

in the general expression for the density of modes ρ_N, Eq. (24), with hyperbolic functions of θ. Making these substitutions gives us

$$\rho_N^{\text{gap}}|_{\beta=\pi+i\theta}=\frac{1}{D}\frac{-(1/2)[\sinh(2N\theta)/\sinh\theta][\eta'+\xi\eta\xi'/(1-\xi^2)]-N\eta\xi'/(1-\xi^2)}{\cosh^2 N\theta+\eta^2[\sinh(N\theta)/\sinh\theta]^2}, \tag{47}$$

which is a general formula for the density of modes anywhere in the first band gap. In general, when we are exactly in the minimum of the band-gap transmittance; $\cos\beta=\xi(\omega)$ has reached either a maximum or minimum value, so that $\xi'=0$. Applying this to Eq. (47) gives us, at MG,

$$\rho_N^{\text{MG}}|_{\xi'=0}=\frac{1}{D}\frac{-(1/2)[\sinh(2N\theta^{\text{MG}})/\sinh\theta^{MG}]\eta'}{\cosh^2 N\theta^{\text{MG}}+\eta^2[\sinh(N\theta^{MG})/\sinh\theta^{MG}]^2}, \tag{48}$$

where $\theta^{\text{MG}}=\cosh^{-1}(-\xi^{\text{MG}})$. For large values of N, the hyperbolic functions can be approximated by exponentials. If this substitution is carried out, the exponential terms of argument $N\theta$ cancel out, leaving

$$\rho_N^{\text{MG}}|_{\xi'=0}\underset{N\to\infty}{\sim}\frac{-1}{Nd}\frac{\eta'\sinh\theta^{\text{MG}}}{\eta^2+\sinh^2\theta^{MG}}. \tag{49}$$

We can see that—in general—ρ_N^{MG} varies asymptotically inversely as N, independently of the unit cell. Equivalently, the group velocity at midgap increases as a linear function of N, eventually becoming "superluminal" [15,16]. For the particular case of the quarter-wave stack, we can evaluate Eqs. (47)–(49) at $\beta=\pi+i\theta^{\text{MG}}$ or $\omega=\omega_0$, using Eq. (43) for d, and Eq. (31) for v^{bulk}, to give the expression

$$\rho_N^{\lambda/4-\text{MG}}=\frac{1}{Nv^{\text{bulk}}}\frac{\sinh N\theta^{\text{MG}}}{\cosh N\theta^{\text{MG}}\sinh\theta^{\text{MG}}}\frac{1}{T_{12}}, \tag{50}$$

where

$$\theta^{\text{MG}}=\cosh^{-1}\left(\frac{n_1^2+n_2^2}{2n_1n_2}\right)=\ln(1/\nu),$$

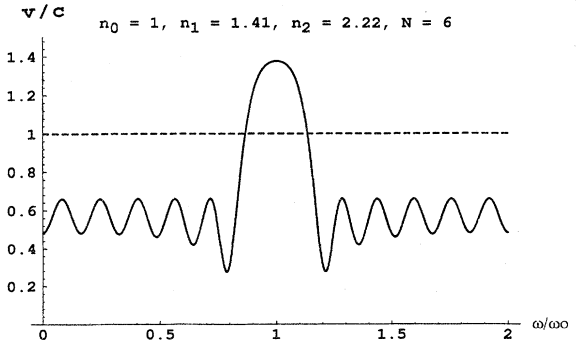

FIG. 8. Plot of the dimensionless group velocity, $v_N/c=(c\rho_N)^{-1}$, Eqs. (24) and (30), vs dimensionless midgap-normalized frequency, ω/ω_0, for a qualitative model of the structure used in the superluminal tunneling-time experiment by Steinberg, Kwiat, and Chiao. For our hypothetical structure we assume 5 periods instead of the $5\frac{1}{2}$ used in the experiment, and we assume air is on both sides, ignoring their substrate. The primary point of interest is the peak of the group velocity v_N/c in the band gap that clearly is greater than the speed of light in a vacuum.

$\nu=n_i/n_j$ where $n_i>n_j$, with $i,j\in(1,2)$, and $T_{12}=4n_1n_1/(n_1+n_2)$ as before. Equation (50) can be simplified by using identities for hyperbolic functions. Doing this we get

$$\rho_N^{\lambda/4-\text{MG}}=\frac{2}{T_{12}v^{\text{bulk}}}\left(\frac{\nu}{\nu^2-1}\right)\left(\frac{\nu^{2N}-1}{\nu^{2N}+1}\right)\frac{1}{N}. \tag{51}$$

For moderate N, the factor $(\nu^{2N}-1)/(\nu^{2N}+1)$ is approximately equal to one (if $\nu=n_i/n_j>1$), so the density of modes is inversely proportional to N, as expected from the general case, Eq. (49). [See Fig. 7(b).]

An experiment was done by Steinberg, Kwiat, and Chiao [15] (SKC) to measure the apparent "superluminal" tunneling velocity of a wave packet through a 1D photonic band-gap structure. They measured this velocity to be $(1.7\pm0.2)c$ at midgap in their experiment. We would like to use our formulation of the group velocity to predict an approximate value for this tunneling velocity. For their experiment, air is the incident material, and a substrate is attached to the other side of a $5\frac{1}{2}$ period PBG structure of the form $(HL)^5H$, where the titanium-oxide "H" layers have high index $n_2=2.22$, and the fused silica in the "L" layers have low index $n_1=1.41$. Up to this point, our formulas for ρ_N and $v_N=1/\rho_N$ assume that the quarter-wave PBG is embedded in a material with an index of refraction that is equal to either of the two indices n_1 or n_2 used in the quarter-wave PBG structure. We can generalize our formula somewhat by allowing the PBG structure to be embedded in a material with an arbitrary index of refraction n_0, say $n_0=1$ (see Appendix C). If this correction is made, using $n_0=1.0$, $n_1=1.41$, and $n_2=2.22$, we calculate a theoretical midgap group velocity of $v^{\text{th}}=1.37c$. (See Fig. 8.) This number is somewhat smaller than the experimental value of $v^{\text{expt}}=(1.7\pm0.2)c$ because we assume that air is on both sides of the structure, that the stack has the form $(HL)^5$ so that $N=5$, and we ignore the substrate. The method that we use in Appendix C to generalize this problem requires that the indices on either side of the PBG structure be the same, hence the term *symmetric sandwiching*. If they are not, the exact solution to the problem becomes a good deal more complex. To calculate the midgap group velocity more accurately, we may simply use the numerical, arbitrary-stack, matrix-transfer method as outlined in Sec. II. Performing this computer calculation gives a much better numerical estimation of the experimentally mea-

sured group velocity, namely, $v^{\text{num}}=1.76c$, well within the experimental error bars of $v^{\text{expt}}=(1.7\pm0.2)c$.

VII. MATCHING THE BANDWIDTH OF $\rho_N^{\lambda/4}$ AT THE BAND-EDGE RESONANCE

As a potential application of the formulas developed thus far, consider the case of a PBG-embedded emitter whose emission rate we would like to enhance at the band-edge resonance. From Fermi's "golden rule," we know that the emission rate is directly proportional to the density of modes, as in Eq. (2). To design our structure, we use the fact that the mode density at the band edge can be quite high. We would like to build a PBG for which the bandwidth, and location of the band-edge peak of the mode density, matches the corresponding parameters of the emitter spectrum. Because n_1 and n_2 are more or less strictly constrained by the physical properties of materials that can be microfabricated with precision, we can also assume that we know their values, or at least some trial set. Given the bandwidth $\Delta\omega$ and location $\bar{\omega}$ of the emitter in frequency space, and the values of n_1 and n_2, we want to solve for values of the midgap frequency ω_0 and number of periods of N, required to actually fabricate the correct stack. We know that for a quarter-wave stack, $\cos\beta=(\cos\pi\bar{\omega}-R_{12})/T_{12}$, where $\bar{\omega}=\omega/\omega_0$. From our arguments about the maxima and minima of ρ_N, we also know the lower band-edge maximum for ρ_N is located between $\beta=[(2N-1)/N](\pi/2)$ and $\beta=[(2N-3)/N](\pi/2)$. Let us also define the quantities

$$\Delta\omega=\frac{\omega_1-\omega_2}{2} \tag{52a}$$

and

$$\bar{\omega}=\frac{\omega_1+\omega_2}{2}, \tag{52b}$$

which are assumed to be the known spectral width and central frequency of our emitter, respectively. Here, ω_1 and ω_2 are the lower and upper limits of the emitter's spectral range, respectively. We can now write two equations relating the two edge frequencies in β space to those in ω space:

$$\cos\left(\pi\frac{\omega_1}{\omega_0}\right)=R_{12}-T_{12}\cos\frac{3\pi}{2N}, \tag{53a}$$

$$\cos\left(\pi\frac{\omega_2}{\omega_0}\right)=R_{12}-T_{12}\cos\frac{\pi}{N}, \tag{53b}$$

where $R_{12}=(n_1-n_2)^2/(n_1+n_2)^2$ and $T_{12}=4n_1n_2/(n_1+n_2)^2$, as before. By adding and then subtracting these two equations we get another pair of equations in $\Delta\omega$ and $\bar{\omega}$, which are

$$\frac{1}{T_{12}}=\frac{1+\cos(\pi/N)\cos[\pi/(2N)]}{1-\cos(\pi\Delta\omega/\omega_0)\cos(\pi\bar{\omega}/\omega_0)}, \tag{54a}$$

$$\frac{1}{T_{12}}=\frac{\sin(\pi/N)\sin[\pi/(2N)]}{\sin(\pi\Delta\omega/\omega_0)\sin(\pi\bar{\omega}/\omega_0)}. \tag{54b}$$

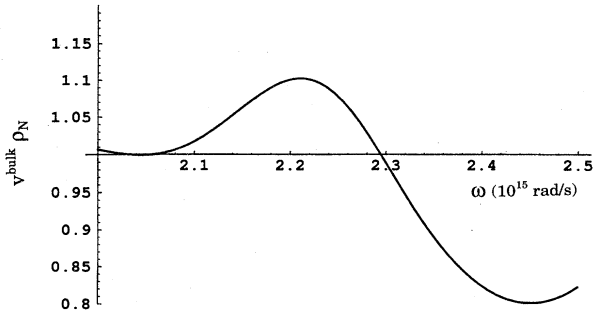

FIG. 9. Plot of the band-edge resonance, Eqs. (24) and (30), for the dimensionless DOM $v^{\text{bulk}}\rho_N$ vs frequency for a quarter-wave stack. Here we have matched the central frequency and frequency width of the band-edge resonance of the DOM, for a quarter-wave stack with fixed n_1 and n_2, to the location and bandwidth of a given spontaneous emitter that is embedded in the PBG. While the peak amplitude of the resonance is relatively small ($\sim$1.12), it is the integrated area, under the resonance and above the line, $v^{\text{bulk}}\rho_N=1$ that is important.

Since T_{12}, $\Delta\omega$, and $\bar{\omega}$ are assumed to be known, we have two equations for the two stack unknowns: ω_0 and N, the midgap frequency and number of periods, respectively. A numerical root-finding routine can now be used to find appropriate values for ω_0 and N, given T_{12}, or equivalently, n_1 and n_2. Let us consider a simple numerical example. Suppose we have $n_1=2.9$, $n_2=3.2$, $\bar{\omega}=2.154\times10^{15}$ rad/s, and $\Delta\omega=0.215\times10^{15}$ rad/s. This corresponds to a quarter-wave stack fashioned from alternating layers of low-index aluminum arsenide with high-index aluminum gallium arsenide, a commonly microfabricated Bragg reflector used in semiconductor spontaneous emission experiments [7]. The spectral width $\Delta\omega$ is chosen to match that of the electron-hole, recombinate spontaneous emission of an active quarter-wave layer of gallium arsenide embedded in the stack. Inserting these values into Eqs. (54) and solving numerically, we find $N=9.23$ and $\omega_0=2.43\times10^{15}$ rad/s. Since N must be an integer, we use $N=9$ and a correspondingly recalibrated $\omega_0=2.45\times10^{15}$ rad/s to plot the DOM curve. From Fig. 9, and by calculating values of ω_1 and ω_2, we observe $\bar{\omega}=2.164\times10^{15}$ rad/s and $\Delta\omega=0.126\times10^{15}$ rad/s. The small difference in the final $\Delta\omega$ and $\bar{\omega}$ from the initial desired values can be attributed to the fact that N had to be rounded to the nearest integer value when the root-finding routine found a noninteger root. When using the root-finding routine, one must be careful to reject nonphysical results such as negative values for N, or a midgap frequency ω_0 that is larger than the upper band edge of the PBG stack.

VIII. SUMMARY AND CONCLUSIONS

We believe this paper illustrates the usefulness of developing and analyzing formulas for transmission, DOM, and group velocity of a simple 1D model of photonic band-gap structures. We have paid special attention to finite periodic structures, in particular the quarter-wave stack. From our results, we have gained a better understanding of some of the

scaling laws inherent in the formulas for transmission, DOM, and group velocity, and we will be able to make accurate predictions concerning the behavior of actual PBG structures.

We began in Sec. II by establishing our definition of the density of modes, $\rho(\omega)\equiv dk/d\omega$, by justifying this convention through its meaning for spontaneous emission in cavity QED. Also in that section, we showed how the DOM can be, in general, constructed from the complex transmission coefficient $t(\omega)$ for an arbitrary, real, 1D dielectric structure, as per Eq. (7). In Sec. III we applied a matrix-transfer method to obtain a formulation for the transmission coefficient $t_N(\omega)$ of an N-period structure in terms of the transmission coefficient t of a unit-cell transmission $T=|t|^2$. We performed the same type of calculation to give us the N-period transmission, $T_N=|t_N|^2$, in terms of the unit cell. These formulas are quite significant, in that we can say something about the transmittance and transmission coefficient of a periodic structure without our knowing much about the unit-cell index of refraction profile $n(x)$. In Sec. IV, we derived our primary result: the DOM $\rho_N(\omega)$ of an N-period potential in terms of the number of periods, parameters of the unit cell, and the Bloch phase β that corresponds to the hypothetical infinite periodic structure constructed from that cell. In Sec. V, we applied the equations derived up to this point to the particular case of a quarter-wave stack, a common 1D PBG structure. In Sec. VI, we investigated some of the interesting properties of the transmittance T_N and the DOM ρ_N. Some of these properties included the behavior of T_N and ρ_N at their maxima and minima, near the band edge, and inside the band gap. It is in Sec. VI that we developed some of the important scaling laws that could be of use for general 1D periodic structures, as well as in the specific case of the quarter-wave stack. Also, in that section we discussed the results of an experiment done to measure midgap tunneling velocity of a pulse, as well as our predictions concerning this superluminal tunneling-time experiment of Steinberg, Kwiat, and Chiao. Finally, in Sec. VII, we applied the equations we have developed thus far to a particular application in which we matched the location and width of the band-edge resonance of the DOM to the known spectrum of an emitter. This paper contains a number of important accomplishments. By developing an equation for the density of modes for a finite periodic structure, we are better equipped to understand the behavior of the DOM and group delay. Furthermore, because of the John-Wang model [3], our results should yield practical approximations for finite 3D PBG structures with nearly spherical BZ zones. There are a number of specific applications for which our results would be readily useful, including spontaneous emission alteration in periodically layered semiconductors [7], nonlinear optical effects, such as gap solitons [11], optical bistability [12], optical limiting and switching [13], and thin-film optical isolators [14].

Finally, we note—due to the isomorphism between the 1D Schrödinger and Maxwell wave equations—that our mode density formulae have direct application in solid-state physics to electron transport in periodically modulated semiconductor quantum wires [22].

ACKNOWLEDGMENTS

The authors would like to acknowledge interesting and useful discussions with G. S. Agarwal, G. Björk, M. J. Bloemer, C. M. Bowden, E. Chai, R. Y. Chiao, J. W. Haus, J. Jacobson, P. G. Kwiat, A. S. Manka, J. E. Sipe, A. M. Steinberg, F. M. Steinberg, M. D. Tocci, and Y. Yamamoto. In addition, J.M.B. and M.S. would like to acknowledge the U.S. Army Missile Command for financial support.

APPENDIX A: PROOF OF FORMULA FOR $\hat{\mathbf{M}}^N$ IN TERMS OF $\hat{\mathbf{M}}$

Here, we prove Eq. (16) in Sec. III by induction. We want to establish the equation

$$\hat{\mathbf{M}}^N=\frac{1}{\sin\beta}[\hat{\mathbf{M}}\sin N\beta-\hat{\mathbf{I}}\sin(N-1)\beta]. \tag{A1}$$

For $N=1$, we have the trivial identity $\hat{\mathbf{M}}=\hat{\mathbf{M}}$. For $N=2$, the equation can be simplified to

$$\hat{\mathbf{M}}^2=2\hat{\mathbf{M}}\cos\beta-\hat{\mathbf{I}}, \tag{A2}$$

which we know to be valid from the Cayley-Hamilton theorem, as per Eq. (15). We then multiply Eq. (A1) by $\hat{\mathbf{M}}$ and simplify the expression

$$\begin{aligned}\hat{\mathbf{M}}^{N+1}&=\frac{1}{\sin\beta}[\hat{\mathbf{M}}^2\sin N\beta-\hat{\mathbf{M}}\sin(N-1)\beta]\\&=\frac{1}{\sin\beta}[2\hat{\mathbf{M}}\cos\beta\sin N\beta-\hat{\mathbf{I}}\sin N\beta\\&\quad-\hat{\mathbf{M}}(\sin N\beta\cos\beta-\cos N\beta\sin\beta)]\\&=\frac{1}{\sin\beta}[\hat{\mathbf{M}}\sin(N+1)\beta-\hat{\mathbf{I}}\sin N\beta].\end{aligned} \tag{A3}$$

We now observe that (A3) and (A1) are precisely the same except that $N\rightarrow N+1$ in Eq. (A3). Since we have shown that the formula is true for $N=1$ and $N=2$, and that the formula is true for $N+1$, given it holds for N, our proof for general N is complete.

APPENDIX B: CONSTRUCTING $\hat{\mathbf{M}}$ FOR THE UNIT CELL

In general, constructing the transfer matrix $\hat{\mathbf{M}}$ for an arbitrary unit cell, $\{n(x):x\in[0,d]\}$, as in Fig. 1, requires the solution of the Helmholtz Eq. (1) in the interval $x\in[0,d)$. This solution will, when the appropriate boundary conditions at $x=0$ and d are imposed, give the transmission coefficient and reflectance coefficients t and r, respectively, needed to construct $\hat{\mathbf{M}}$ as per the general formula, Eq. (16). For a large class of functions $n(x)$, the solution to Eq. (1) is known in terms of relatively simple special functions. For example, if the dielectric profile $\epsilon(x)$ is linear, i.e., $n^2(x)=\epsilon(x)=mx+b$, then $\hat{\mathbf{M}}$ is expressible in terms of Airy functions.

For a large class of practical problems, the unit cell has the form of a series of steps, namely, $n(x)=n_i$, where $x\in[x_{i-1},x_i)$; with $i\in\{1,\ldots,m\}$—taking $x_0=0$ and $x_m=d$, and also assuming each n_i is a dispersionless constant. The transfer matrix for such an index potential will always be the product of matrices of only two types. The first is a discontinuity matrix $\hat{\mathbf{\Delta}}_{ij}$ that transfers the field amplitude left to

right across the $n_i \rightarrow n_j$ interface. The second is a propagation matrix $\hat{\mathbf{\Pi}}(p_i)$, where $p_i \equiv n_i a_i(\omega/c)$ is the phase that accumulates as the field propagates left to right a distance $a_i \equiv |x_i - x_{i-1}|$ in the constant n_i region between the $(i-1)$st and ith interfaces. These matrices have the form [23]

$$\hat{\mathbf{\Delta}}_{ij} \equiv \begin{pmatrix} \delta_{ij}^{+} & \delta_{ij}^{-} \\ \delta_{ij}^{-} & \delta_{ij}^{+} \end{pmatrix} \tag{B1a}$$

and

$$\hat{\mathbf{\Pi}}(p_i) \equiv \begin{pmatrix} e^{ip_i} & 0 \\ 0 & e^{-ip_i} \end{pmatrix}, \tag{B1b}$$

respectively, where $\delta_{ij}^{\pm} \equiv \frac{1}{2}(1 \pm n_i/n_j)$. By comparing Eq. (B1a) to the general transfer matrix form given by Eq. (11), we see that $\delta_{ij}^{+} = 1/t_{ij}$ and $\delta_{ij}^{-} = r_{ij}/t_{ij}$, where t_{ij} and r_{ij} are the $n_i \rightarrow n_j$ interface transmission and reflectance coefficients, given by [19]

$$t_{ij} = \frac{2n_j}{n_i + n_j} \tag{B2a}$$

and

$$r_{ij} = \frac{n_i - n_j}{n_i + n_j} = -r_{ji}. \tag{B2b}$$

We define special double-transmission and double-reflection coefficients, T_{12} and R_{12}, by

$$T_{12} \equiv t_{12}t_{21} = \frac{4n_1 n_2}{(n_1 + n_2)^2}, \tag{B3a}$$

$$R_{12} \equiv -r_{12}r_{21} = \left(\frac{n_1 - n_2}{n_1 + n_2} \right)^2, \tag{B3b}$$

such that $T_{12} + R_{12} \equiv 1$. The $\hat{\mathbf{\Delta}}$ matrices have the following useful proper ties:

$$\hat{\mathbf{\Delta}}_{ij}\hat{\mathbf{\Delta}}_{kl} = \hat{\mathbf{\Delta}}_{kl}\hat{\mathbf{\Delta}}_{ij} \quad \text{(commutativity)}, \tag{B4a}$$

$$\hat{\mathbf{\Delta}}_{ij}\hat{\mathbf{\Delta}}_{jk} = \hat{\mathbf{\Delta}}_{ik} \quad \text{(transitivity)}, \tag{B4b}$$

$$\hat{\mathbf{\Delta}}_{ij}\hat{\mathbf{\Delta}}_{ji} = \hat{\mathbf{I}} \quad \text{(identity)}. \tag{B4c}$$

The $\hat{\mathbf{\Pi}}$ obey

$$\hat{\mathbf{\Pi}}(0) = \hat{\mathbf{\Pi}}(p)\hat{\mathbf{\Pi}}(-p) = \hat{\mathbf{I}} \quad \text{(identity)}, \tag{B5a}$$

$$\hat{\mathbf{\Pi}}(p + 2\pi) = \hat{\mathbf{\Pi}}(p) \quad \text{(periodicity)}. \tag{B5b}$$

Using these simple matrices, an arbitrary unit-cell matrix $\hat{\mathbf{M}}$ for a steplike index profile $n(x)$ can be constructed. To illustrate how this is done, we now construct $\hat{\mathbf{M}}$ for a two-layer unit cell to be used in constructing a simple dielectric stack with alternating indices n_1 and n_2. Consider the index profile

$$n(x) = \begin{cases} n_1, & x \in [0,a) \\ n_2 & x \in [a, a+b), \end{cases} \tag{B6}$$

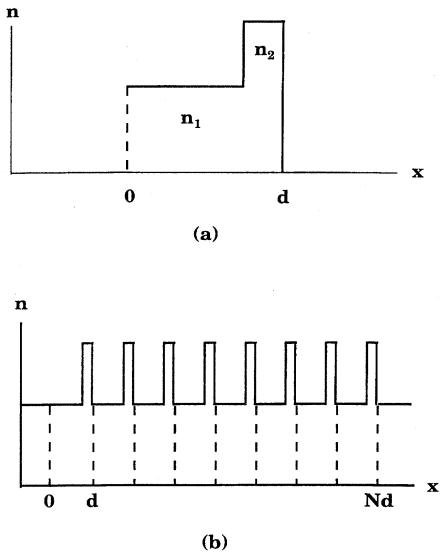

FIG. 10. Here we show how to use the elementary transfer matrices of Appendix B to construct an N-period dielectric stack, composed of two-layer unit cells. In (a) we represent the unit-cell matrix product, Eq. (B7). This unit cell generates the N-period stack in (b), as per Eq. (16) for $\hat{\mathbf{M}}^N$.

shown in Fig. 10(a). Now we want to choose our matrices for $\hat{\mathbf{M}}$ so that $\hat{\mathbf{M}}^N$ is the correct matrix for an N-period, multilayer stack. The choice is

$$\hat{\mathbf{M}}^{-1} \equiv \hat{\mathbf{\Pi}}(p)\hat{\mathbf{\Delta}}_{12}\hat{\mathbf{\Pi}}(q)\hat{\mathbf{\Delta}}_{21} \tag{B7}$$

or

$$\hat{\mathbf{M}} \equiv \hat{\mathbf{\Delta}}_{12}\hat{\mathbf{\Pi}}(-q)\hat{\mathbf{\Delta}}_{21}\hat{\mathbf{\Pi}}(-p), \tag{B8}$$

where $p \equiv n_1 a\omega/c$ and $q \equiv n_2 b\omega/c$, where a and b are the layer thicknesses $(a+b=d)$, and ω the frequency of light impinging on the stack. Recall that $\hat{\mathbf{M}}$, as per Eq. (10), propagates right to left, whereas the $\hat{\mathbf{\Pi}}$ and $\hat{\mathbf{\Delta}}$—defined above—propagate left to right, hence the need for starting with $\hat{\mathbf{M}}^{-1}$, and using the matrix identity $(\hat{\mathbf{A}}\hat{\mathbf{B}})^{-1} \equiv \hat{\mathbf{B}}^{-1}\hat{\mathbf{A}}^{-1}$, as well as Eqs. (B4c) and (B5a). The index potential corresponding to $\hat{\mathbf{M}}^N$ is shown in Fig. 10(b). Note that, in order to be consistent with Eq. (B8), this potential must be "sandwiched" between the half-infinite regions $(-\infty,0)$ and $[Nd,\infty)$, both of index n_1. Now, carrying out the matrix product for $\hat{\mathbf{M}}$, Eq. (B8), using the definition of $\hat{\Delta}$ and $\hat{\mathbf{\Pi}}$, Eqs. (B1a) and (B1b), we arrive at the two-layer unit cell $\hat{\mathbf{M}}$, whose elements are

$$\frac{1}{t} = M_{11} = \delta_{12}^{+}\delta_{21}^{+}e^{i(p+q)} + \delta_{12}^{-}\delta_{21}^{-}e^{i(p-q)}, \tag{B9a}$$

$$\frac{r}{t} = M_{21} = \delta_{12}^{+}\delta_{21}^{-}e^{-i(p+q)} + \delta_{12}^{-}\delta_{21}^{+}e^{-i(p-q)}, \tag{B9b}$$

where $M_{22} = M_{11}^{*}$, and $M_{12} = M_{21}^{*}$, as per Eq. (11). We have $p \equiv n_1 a\omega/c$, $q \equiv n_2 b\omega/c$, and $\delta_{ij}^{\pm} \equiv (1 \pm n_i/n_j)/2$, as before.

Note that at this point these formulas are valid for an arbitrary two-layer unit cell. Making the additional assumption that

$$p=q=\frac{2\pi}{4}\frac{\omega}{\omega_0}\equiv\frac{\pi\tilde{\omega}}{2}, \tag{B10}$$

where $\tilde{\omega}=\omega/\omega_0$, requires that light at midgap frequency ω_0 accumulates $\pi/2$ radians of phase in each of the n_1 or n_2 layers. This demand gives us, of course, the *quarter-wave stack condition* [19].

APPENDIX C: SYMMETRIC SANDWICHING

Here, we show how our formulation for ρ_N and group velocity $v_N=1/\rho_N$ can be generalized to allow the PBG structure to be embedded in a material with arbitrary index of refraction n_0. To achieve our result, we simply "sandwich" the previously described transfer matrix $\hat{\mathbf{M}}^N$ between the appropriate discontinuity matrices $\hat{\mathbf{\Delta}}_{01}$ and $\hat{\mathbf{\Delta}}_{10}$, as defined in Appendix B. Referring back to Eq. (16), we have

$$\hat{\mathbf{\Delta}}_{01}\hat{\mathbf{M}}^N\hat{\mathbf{\Delta}}_{10}=\frac{1}{\sin\beta}\left[\hat{\mathbf{\Delta}}_{01}\hat{\mathbf{M}}\hat{\mathbf{\Delta}}_{10}\sin N\beta - \hat{\mathbf{\Delta}}_{01}\hat{\mathbf{I}}\hat{\mathbf{\Delta}}_{10}\sin(N-1)\beta\right]. \tag{C1}$$

We now need to calculate the quantities $\hat{\mathbf{\Delta}}_{01}\hat{\mathbf{M}}\hat{\mathbf{\Delta}}_{10}$ and $\hat{\mathbf{\Delta}}_{01}\hat{\mathbf{I}}\hat{\mathbf{\Delta}}_{10}$. We know that a general transfer matrix has the form given in Eq. (11). After multiplying together the matrices $\hat{\mathbf{\Delta}}_{01}\hat{\mathbf{I}}\hat{\mathbf{\Delta}}_{10}$ as per Appendix B, we get the identity matrix $\hat{\mathbf{I}}$ as a result, so the second term in Eq. (C1) remains unchanged. Next, we calculate the quantity $\hat{\mathbf{\Delta}}_{01}\hat{\mathbf{M}}\hat{\mathbf{\Delta}}_{10}\equiv\hat{\mathbf{M}}_{\#}$. If we multiply the matrices together and extract the $(\hat{\mathbf{M}}_{\#})_{11}$ element, using Eq. (11), we get the relation

$$\frac{1}{t_{\#}}=\frac{1}{t_{01}}\left[\frac{1}{t}+2ir_{01}\mathrm{Im}\left(\frac{r}{t}\right)-\frac{R_{01}}{t^*}\right], \tag{C2}$$

where $T_{01}=t_{01}t_{10}=4n_0n_1/(n_0+n_1)^2$, $r_{01}=(n_0-n_1)/(n_0+n_1)$, and $R_{01}\equiv|r_{01}|^2$, are the $n_0\rightarrow n_1$ interface transmission and reflection coefficients, as per Eqs. (B2) and (B3). Here, t and r are the unit-cell coefficients, as before. At this point we note that the net effect of symmetric sandwiching on $\hat{\mathbf{M}}^N$ is to modify the value of t to $t_{\#}$ for the effective unit cell. Therefore, if we can calculate the modified values of $\xi_{\#}$, $\xi'_{\#}$, $\eta_{\#}$, and $\eta'_{\#}$, from $t_{\#}$, the equations for T_N and ρ_N, Eqs. (19) and (24), respectively, will be valid for these modified unit-cell parameters, giving the symmetric-sandwiched quantities $T_N^{\#}$ and $\rho_N^{\#}$. Using Eq. (C2), and following a procedure similar to that used in Sec. IV, we can derive $x_{\#}$, $y_{\#}$, $\xi_{\#}\equiv x_{\#}/(x_{\#}^2+y_{\#}^2)$, and $\eta_{\#}\equiv y_{\#}/(x_{\#}^2+y_{\#}^2)$ from $t_{\#}\equiv x_{\#}+iy_{\#}$. For simplicity, we also define

$$f=2r_{01}\mathrm{Im}\left[\frac{r}{t}\right]. \tag{C3}$$

Doing this, we find that the formulas relating ξ and η, for the original unit cell, to $\xi_{\#}$ and $\eta_{\#}$, for the effective unit cell in the sandwiched case, are

$$\xi_{\#}=\xi, \tag{C4a}$$

$$\eta_{\#}=\frac{1}{T_{01}}\left[(1+R_{01})\eta-f\right]. \tag{C4b}$$

The final thing we have to do then is to calculate f, which entails finding $1/t$. To do this, we use the transfer matrix for a quarter-wave stack unit cell. The complete transfer matrix for the unit cell is generated by multiplying together the appropriate propagation and discontinuity matrices, as outlined in Appendix B. For a quarter-wave unit cell we have, from Eqs. (B9b) and (B10),

$$\frac{r}{t}=\frac{r_{21}}{T_{21}}(1-e^{-i\pi\tilde{\omega}}), \tag{C5}$$

where $\tilde{\omega}\equiv\omega/\omega_0$, with ω_0 at midgap. From this, we are able to generate f:

$$f=2\frac{r_{01}r_{21}}{T_{12}}\sin\pi\tilde{\omega}, \tag{C6}$$

Since we have now found f, we have all the information for computing $\eta_{\#}$ and also $\eta'_{\#}$, via Eq. (C4b). Since $\xi_{\#}=\xi$, $\xi'_{\#}=\xi'$, from Eq. (C4a), we are prepared to calculate $\rho_N^{\#}$ for the symmetric sandwich, using the effective $t_{\#}$, Eq. (C2), instead of t in Eq. (24) for ρ_N.

Note that in the case of an *asymmetric* sandwich, $\hat{\mathbf{M}}_{\#}^N=\hat{\mathbf{\Delta}}_{01}\hat{\mathbf{M}}^N\hat{\mathbf{\Delta}}_{13}$, with $n_0\neq n_3$, this trick *cannot* be used since $\hat{\mathbf{\Delta}}_{01}\hat{\mathbf{I}}\hat{\mathbf{\Delta}}_{13}=\hat{\mathbf{\Delta}}_{03}\neq\hat{\mathbf{I}}$, in Eq. (C1). In this case the formula for $\rho_N^{\#}$ must be rederived from scratch, or a numerical matrix-multiplication scheme should be used, as per Sec. II.

[1] *Development and Applications of Materials Exhibiting Photonic Band Gaps*, edited by C. M. Bowden, J. P. Dowling, and H. O. Everitt, special issue of J. Opt. Soc. Am. B **10**, 279 (1993); *Principles and Applications of Photonic Bandgap Structures*, edited by J. W. Haus and G. Kurizki, special issue of J. Mod. Opt. **41**, 345 (1994); J. D. Joannopoulos, R. D. Mead, and J. N. Winn, *Photonic Crystals* (Princeton University Press, Princeton, 1995).

[2] E. Yablonovitch and K. M. Leung, Physica B **175**, 81 (1991); H. S. Sözüer, and J. W. Haus, J. Opt. Soc. Am. B **10**, 296 (1993); H. S. Sözüer and J. P. Dowling, J. Mod. Opt. **41**, 231 (1994); K. M. Ho *et al.*, Solid State Commun. **89**, 413 (1994).

[3] S. John and J. Wang, Phys. Rev. B **43**, 12 772 (1991).

[4] J. P. Dowling and C. M. Bowden, Phys. Rev. A **46**, 612 (1992).

[5] J. P. Dowling and C. M. Bowden, J. Mod. Opt. **41**, 345 (1994).

[6] W. Heitler, *The Quantum Theory of Radiation*, 3rd ed. (Dover, New York, 1984), Chap. IV, Sec. 14.

[7] M. D. Tocci, M. Scalora, M. J. Bloemer, J. P. Dowling, and C. M. Bowden, Phys. Rev. A **53**, 2799 (1996); M. Scalora, R. J. Flynn, S. B. Reinhardt, R. L. Fork, M. D. Tocci, M. J. Bloemer, C. M. Bowden, H. Ledbetter, and J. P. Dowling (unpublished).

[8] Ph. A. Martin, Acta Phys. Austriaca, Suppl. **23**, 159 (1981); M. Sassoli de Bianchi and M. Di Ventra, J. Math. Phys. **36**, 1753 (1995).

[9] D. W. L. Sprung, H. Wu, and J. Martorell, Am. J. Phys. **61**, 1118 (1993); M. G. Rozman, P. Reineker, and R. Tehver, Phys. Lett. A **187**, 127 (1994).

[10] J. P. Dowling, M. Scalora, M. J. Bloemer, and C. M. Bowden, J. Appl. Phys. **75**, 1896 (1994).

[11] C. M. deSterke and J. E. Sipe, Phys. Rev. A **42**, 2858 (1990); **38**, 5149 (1988).

[12] B. Acklin, M. Cada, J. He, and M.-A. Dupertuis, Appl. Phys. Lett. **63**, 2177 (1993); G. Assanto and G. I. Stegeman, *ibid.* **56**, 2285 (1990).

[13] M. Scalora, J. P. Dowling, C. M. Bowden, and M. J. Bloemer, Phys. Rev. Lett. **73**, 1368 (1994); N. D. Sankey, D. F. Prelewitz, and T. G. Brown, Appl. Phys. Lett. **60**, 1427 (1992).

[14] M. Scalora, J. P. Dowling, and C. M. Bowden, J. Appl. Phys. **76**, 2023 (1994); M. D. Tocci, M. J. Bloemer, M. Scalora, J. P. Dowling, and C. M. Bowden, Appl. Phys. Lett. **66**, 2324 (1995).

[15] A. M. Steinberg and R. Y. Chiao, Phys. Rev. A **51**, 3525 (1995); **49**, 3283 (1994); A. M. Steinberg, P. G. Kwiat, and R. Y. Chiao, Phys. Rev. Lett. **71**, 708 (1993).

[16] M. Scalora, J. P. Dowling, A. S. Manka, C. M. Bowden, and J. W. Haus, Phys. Rev. A **52**, 726 (1995).

[17] See, for example, C. Kittel, *Quantum Theory of Solids* (Wiley, New York, 1987), Chap. 5; F. K. Richtmayer, E. H. Kennard, and J. N. Cooper, *Introduction to Modern Physics*, 6th ed. (McGraw-Hill, New York, 1969), Sec. 5.6.

[18] J. P. Dowling, Found. Phys. **23**, 895 (1993); F. B. Seeley, J. E. Alexander, R. W. Connaster, J. S. Conway, and J. P. Dowling, Am. J. Phys. **61**, 545 (1993).

[19] A. Yariv and P. Yeh, *Optical Waves in Crystals* (Wiley, New York, 1984), Sec. 1.5; P. Yeh, *Optical Waves in Layered Media* (Wiley, New York, 1988), Chap. 6; J. Opt. Soc. Am. A **2**, 568 (1985).

[20] This theorem can be found in any linear algebra book; see, for example, A. L. Rabenstein, *Elementary Differential Equations with Linear Algebra*, 3rd ed. (Academic, New York, 1982), Sec. 4.5.

[21] E. R. Brown and O. B. McMahon, Appl. Phys. Lett. **67**, 2138 (1995); P. M. Bell, J. B. Pendry, L. M. Moreno, and A. J. Ward, Comput. Phys. Commun. **85**, 306 (1995).

[22] H. Wu, W. L. Sprung, J. Martorell, and S. Klarsfeld, Phys. Rev. B **44**, 6351 (1991).

[23] J. S. Walker and J. Gathright, Am. J. Phys. **62**, 408 (1994).